Monatshefte für Chemie (2002)
DOI 10.1007/s00706-002-0492-9

Monatshefte für Chemie
Chemical Monthly
Printed in Austria

Invited Review

Spin Transition of 1D, 2D and 3D Iron(II) Complex Polymers The Tug-of-War between Elastic Interaction and a Shock-Absorber Effect

Petra J. van Koningsbruggen[1,*], **Matthias Grunert**[2],
and **Peter Weinberger**[2]

[1] Institute for Inorganic and Analytical Chemistry, Johannes Gutenberg University, D-55099 Mainz, Germany
[2] Institute of Applied Synthetic Chemistry, Vienna University of Technology, A-1060 Vienna, Austria

Received April 8, 2002; accepted April 18, 2002

Summary. The structures of linear chain Fe(II) spin-crossover compounds of α,β- and α,ω-bis(tetrazol-1-yl)alkane type ligands are described in relation to their magnetic properties. The first threefold interlocked 3-D catenane Fe(II) spin-transition system, [μ-tris(1,4-bis(tetrazol-1-yl)butane-N1,N1′) iron(II)] bis(perchlorate), will be discussed. An analysis is made among the structures and the cooperativity of the spin-crossover behaviour of polynuclear Fe(II) spin-transition materials.

Keywords. Spin-crossover; High-spin; Low-spin; Fe(II); Tetrazole; Polynuclear compounds; Chain; Catenane.

Introduction

Spin-crossover materials are increasingly investigated due to their perceived technological importance, which is based on their possible application as molecular-based memory devices and displays [1–3]. Especially, Fe(II) spin-crossover compounds exhibit favourable response functions towards a change in temperature or pressure, and also upon light irradiation [1–15]: the thereby occurring interconversion from low-spin (LS; $S = 0$) and high-spin (HS; $S = 2$) represents the magnetic response, and moreover, it is frequently associated with a pronounced thermochromic effect. This is, for instance, the case for the extensively studied

---

* Corresponding author. E-mail: koning@iacgu7.chemie.uni-mainz.de

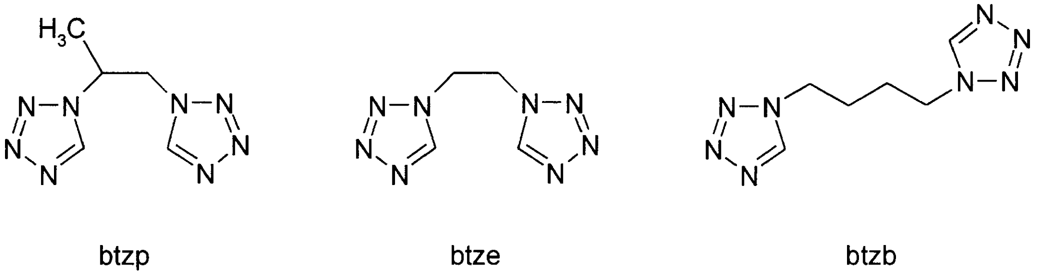

Fig. 1. 1,2-bis(tetrazol-1-yl)propane (*btzp*), 1,2-bis(tetrazol-1-yl)ethane (*btze*) and 1,4-bis(tetrazol-1-yl)butane (*btzb*)

[Fe(1-propyl-tetrazole)$_6$](BF$_4$)$_2$ [12–17], which shows very abrupt spin transitions, a feature which may very well be described by the model of elastic interactions [18], and even thermal hysteresis, which is due to a first order crystallographic phase transition [19]. Generally, the occurrence of thermal hysteresis in mononuclear Fe(II) spin-crossover compounds may also be brought about by strong intermolecular interactions resulting from the presence of an important hydrogen bonding network [20, 21] or extended π–π interactions [22, 23]. Unfortunately, these features invoked to be responsible for thermal hysteresis are extremely difficult to control, hence alternative strategies involving polynuclear Fe(II) compounds have been applied during the last decade. This quest for polynuclear Fe(II) spin-crossover compounds has been motivated by the fact that an efficient propagation of the molecular distortions originating from the Fe(II) spin transition through the crystal lattice is enhanced by the direct covalent intramolecular bonds.

Our approach is based on the use of α,β- and α,ω-bis(tetrazol-1-yl)alkane type ligands. This paper deals with the comparison of the structural features in relation to the Fe(II) spin-crossover properties of various linear chain Fe(II) spin-crossover compounds obtained with the ligands 1,2-bis(tetrazol-1-yl)propane (abbreviated as *btzp*) and 1,2-bis(tetrazol-1-yl)ethane (abbreviated as *btze*) (Fig. 1). These structures will also be compared with the crystallographic data of a related Cu(II) linear chain of *btze*.

It will also be shown that increasing the length of the alkyl spacer in such a way as to yield 1,4-bis(tetrazol-1-yl)butane (abbreviated as *btzb*) (Fig. 1), proves to be a valuable tool in determining the dimensionality of the Fe(II) spin-crossover material. The Fe(II) spin-crossover properties of this polynuclear compound will be discussed and compared to these reported for other polynuclear Fe(II) spin-transition materials. Special emphasis is given to the factors leading to the cooperativity of the Fe(II) spin-crossover behaviour in these various systems.

Results

Spin-Crossover Behaviour and Structure of [Fe(btzp)$_3$](ClO$_4$)$_2$

[Fe(*btzp*)$_3$](ClO$_4$)$_2$ represents the first structurally characterized Fe(II) linear-chain compound exhibiting thermal spin-crossover [24]. It shows gradual spin-crossover behaviour with a transition temperature $T_{1/2}$, *i.e.* where equivalent amounts of spin

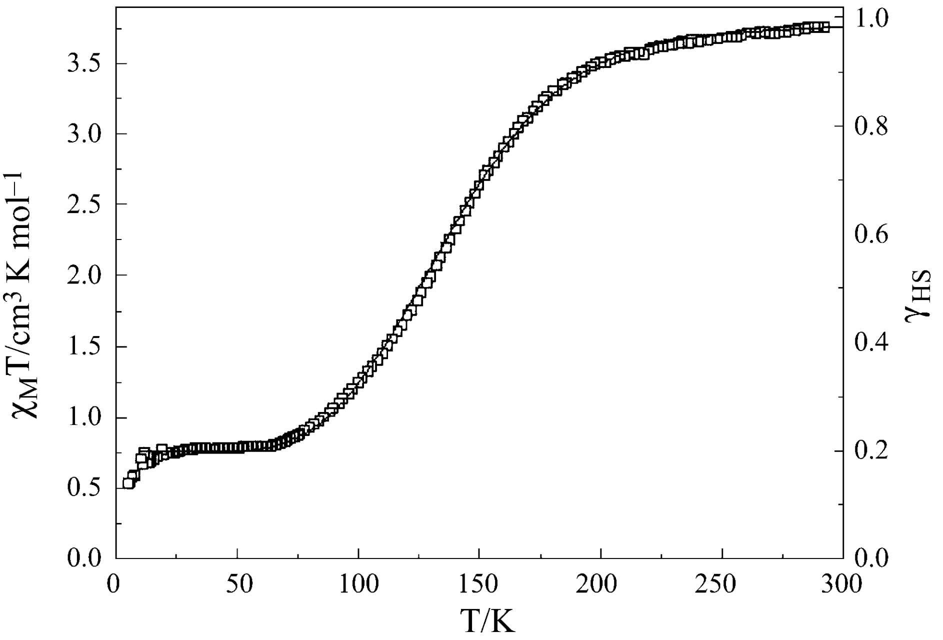

Fig. 2. $\chi_M T$ and γ_{HS} *versus* T plots both in the cooling and warming mode for [Fe(*btzp*)$_3$](ClO$_4$)$_2$ in the 4.2–300 K temperature range [24]

switching Fe(II) ions in low-spin and high-spin forms are present, of 148 K, as evidenced by variable temperature magnetic susceptibility measurements and ^{57}Fe *Mössbauer* spectroscopy. The magnetic behaviour of [Fe(*btzp*)$_3$](ClO$_4$)$_2$ is shown in Fig. 2 in the form of the $\chi_M T$ *versus* T plot, χ_M being the molar magnetic susceptibility per iron(II) ion and T the temperature. At higher temperatures, the spin-crossover is fairly complete yielding 100% of high-spin Fe(II) ions, whereas at 60 K a mixture of low-spin and high-spin Fe(II) ions, with the molar fractions 0.80 and 0.20, respectively, could be detected. The presence of Fe(III) could be ruled out based on the ^{57}Fe *Mössbauer* spectroscopy data [24]. The solid line shown in Fig. 2 shows the fraction of high-spin Fe(II) species γ_{HS} as function of the temperature, as derived from the regular solution model. The transition does not show any hysteresis, since the $\chi_M T$ *versus* T curves recorded at decreasing and increasing temperatures are identical.

Most interestingly, [Fe(*btzp*)$_3$](ClO$_4$)$_2$ undergoes light-induced excited spin-state trapping (LIESST effect). To the best of our knowledge, this is the first and only one-dimensional Fe(II) spin-crossover compound behaving this way.

The structure has been solved at 200 K and 100 K by single-crystal X-ray crystallography. A view of the cationic iron(II) linear chain is depicted in Fig. 3. The space group at 100 K and 200 K is P$\bar{3}$c1. The asymmetric unit consists of an iron(II) ion and one half of the *btzp* ligand. The C3 of the 1,2-propane linkage is crystallographically disordered and yielded two partially occupied positions. This originates from the use of the racemic mixture of the ligand in the synthesis of the Fe(II) compound. A disordered perchlorate anion completes this asymmetric unit. The Fe(II) ion lies on the threefold axis and has an inversion center. It is in an octahedral environment formed by six crystallographically related *N*4 coordinating

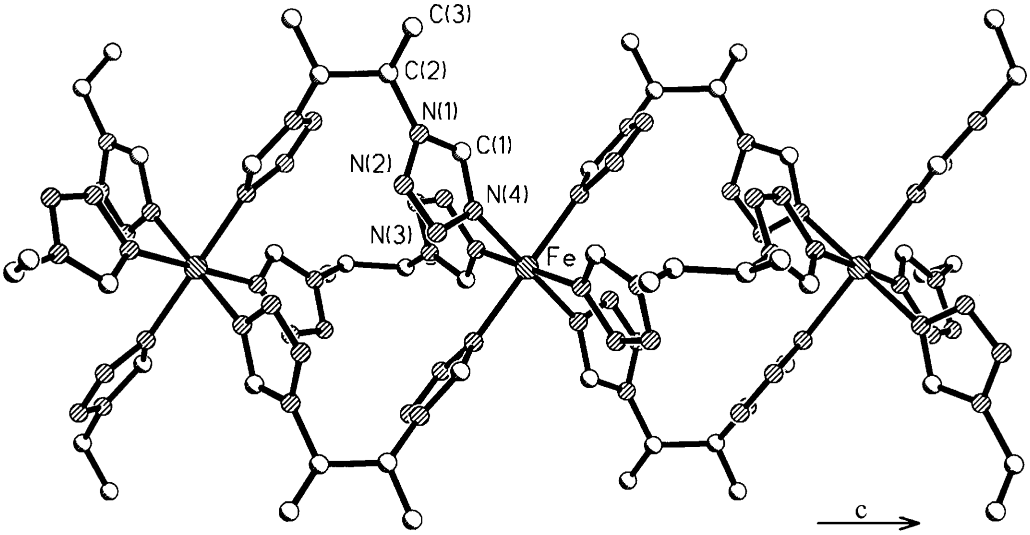

Fig. 3. View of the structure of $[Fe(btzp)_3](ClO_4)_2$ perpendicular to the *c*-axis at 100 K (adapted from [24])

1-tetrazole moieties. The almost perfect O_h symmetry for the FeN_6 core is therefore present in the high-spin and low-spin state. The latter feature could also be confirmed by the ^{57}Fe *Mössbauer* spectra, showing a singlet, the characteristic signature for one of the rare cases of cubic local symmetry for an Fe(II) ion in the low-spin state. The Fe–N4 distance of 2.164(4) Å at 200 K corresponds to the value expected for an Fe(II) ion in the high-spin state [5]. At 100 K, the Fe–N4 distance is equal to 2.038(4) Å, which is a typical value for an Fe(II) ion in the LS state [5]. The Fe–N4 distance decreases by 6% upon the spin conversion, which corresponds to the values found for other spin-crossover compounds [5]. The Fe(II) octahedron is very slightly distorted in the high-spin state with two sets of bond angles N–Fe–N of 91.1(2)° and 88.9(2)°. However, as expected, it is quasi regular in the low-spin state with bond angles N–Fe–N of 90.8(2)° and 89.2(2)°. The Fe(II) ions are linked by a bridge composed of three bis(tetrazole) ligands, leading to a regular linear chain running along the *c*-axis with Fe–Fe separations of 7.422(1) Å at 200 K and 7.273(1) Å at 100 K. The *btzp* ligand has a bent *syn* conformation, which is illustrated by the torsion angle $N1–C1–C2^a–N1^a$ ($a = y, x, 0.5 - z$) of $-34(1)°$ at 200 K and of $-35(1)°$ at 100 K. A projection of the structure at 200 K perpendicular to the *b*-axis is shown in Fig. 4. The space-filling of the Fe(II) chains shows a hexagonal motif. In turn, the linear chains are packed in such a way as to form hexagonal cavities in the *ab* plane. The non-coordinated perchlorate anions reside in the voids of this molecular architecture. There are no intermolecular contacts between the linear chains. The apparent contacts between C3 atoms originating from different chains may be attributed to the statistical disorder of these C3 atoms.

The largest change in cell dimensions due to the spin transition amounts to 2.1% over the temperature range 100–200 K, and was found for the *c*-axis, *i.e.*, the chain axis. The changes in the *a*- and *b*-axes are considerably smaller (0.6%). The actual cell volume decreases by 3.3% in the temperature range from 200 to 100 K.

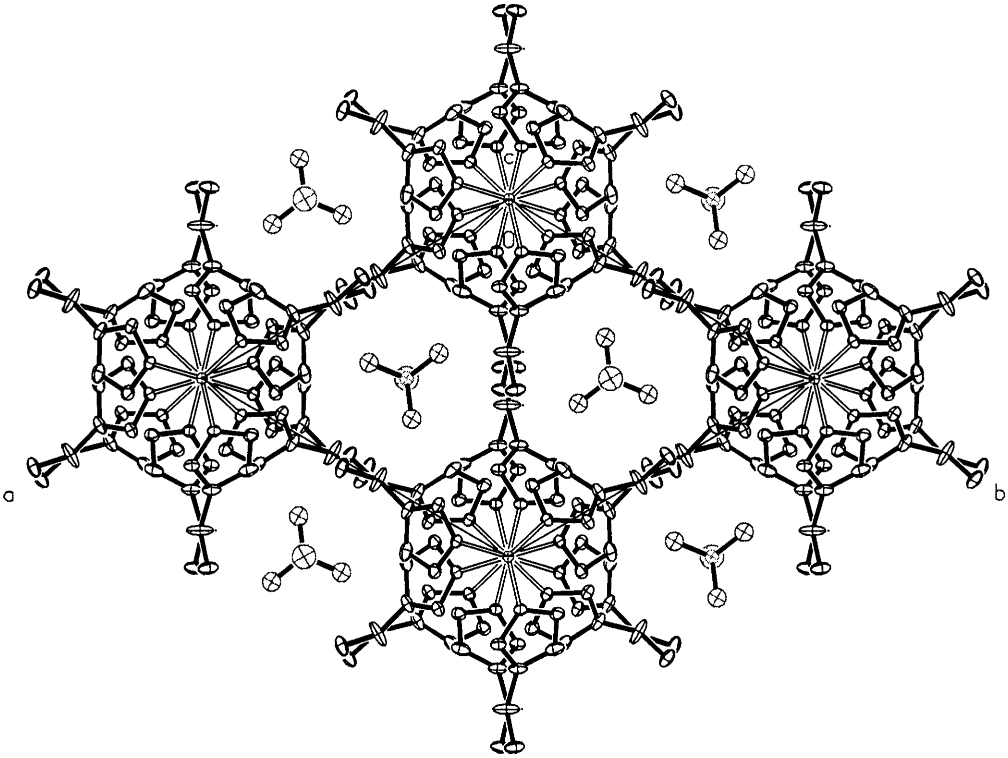

Fig. 4. View of the crystal structure of [Fe(*btzp*)$_3$](ClO$_4$)$_2$ down the *c*-axis at 100 K (adapted from [24])

The volume change per Fe(II) ion is 25.4 Å^3, which falls in the range normally observed [5].

Spin-Crossover Behaviour and Structure of [Fe(btze)$_3$](BF$_4$)$_2$

Continuing this research, we investigated in which way the variation of a 1,2-propane linkage towards a 1,2-ethane linkage between the tetrazole moieties influences the structural features. Recently, we reported [Fe(1,2-bis(tetrazol-1-yl) ethane)$_3$](BF$_4$)$_2$, a comparable Fe(II) spin transition linear chain with a somewhat more abrupt spin transition centered at 140 K [25]. The variable temperature magnetic susceptibility measurements (Fig. 5), as well as the ^{57}Fe *Mössbauer* spectroscopy study gave evidence for an Fe(II) spin-crossover behaviour that is complete at higher temperatures, however, with a residual Fe(II) high-spin fraction of about 9.3% at lower temperatures. Superimposed on this spin-crossover behaviour of the Fe(II) ions, the ^{57}Fe *Mössbauer* spectra recorded over the whole temperature range also revealed the presence of a small fraction (7%) of high-spin Fe(III) ions.

The structure of [Fe(1,2-bis(tetrazol-1-yl)ethane)$_3$](BF$_4$)$_2$ has been determined in the trigonal space group P$\bar{3}$c1 at 296, 200, 150 and 100 K, and corresponds to these described for [tris(1,2-bis(tetrazol-1-yl)propane)iron(II)] bisperchlorate [24]. Also in this case, paramount disorder has been encountered in the crystal structure, however, of a different nature than for the former Fe(II) linear chain compound.

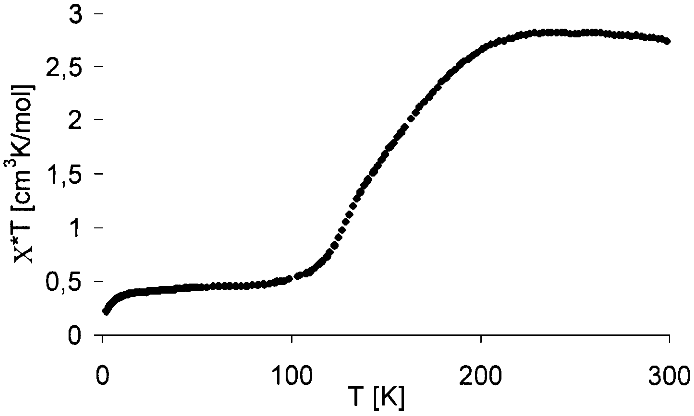

Fig. 5. Temperature dependent magnetic susceptibility of [Fe(*btze*)$_3$](BF$_4$)$_2$ [25]

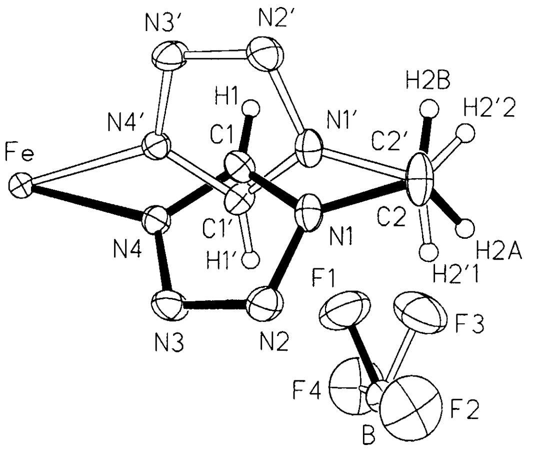

Fig. 6. Asymmetric unit of the structure of [Fe(*btze*)$_3$](BF$_4$)$_2$ ($T = 296$ K) showing two alternatively occupied sets of atoms linked by full/open bonds, as used in the final structure refinement [25]

This may best be viewed from Fig. 6 showing the asymmetric unit of the structure of [Fe(*btze*)$_3$](BF$_4$)$_2$. The asymmetric unit consists of an iron(II) ion, one half of the *btze* ligand and a tetrafluoroborate anion. The *btze* ligand adopts two orientations, characterized by two sets of atoms that are related by pseudo-symmetry and distinguished by unprimed and primed atoms. The refined site occupation factors for split positions were almost 0.5, *i.e.* 0.498(3). Also in this case, the geometry formed by the six N-donating *btze* ligands about the Fe(II) ion is almost perfectly octahedral. The Fe–N bond lengths are markedly temperature dependent: At room temperature the Fe–N bond length of 2.182(1) Å corresponds to a typical Fe(II) ion in high-spin state [5]. After a small contraction to 2.160(1) Å at 200 K, there is a significant decrease to 2.095(2) Å at 150 K and to 2.004(1) Å at 100 K. This is accompanied by a concomitant change in the colour of the crystal from colorless (296 and 200 K) to an intense pink (150 K and 100 K). The short Fe–N distance at 100 K is consistent with the transition to the low-spin state [5]. Three *btze* ligands link the Fe(II) centers to form cationic chains running parallel to the

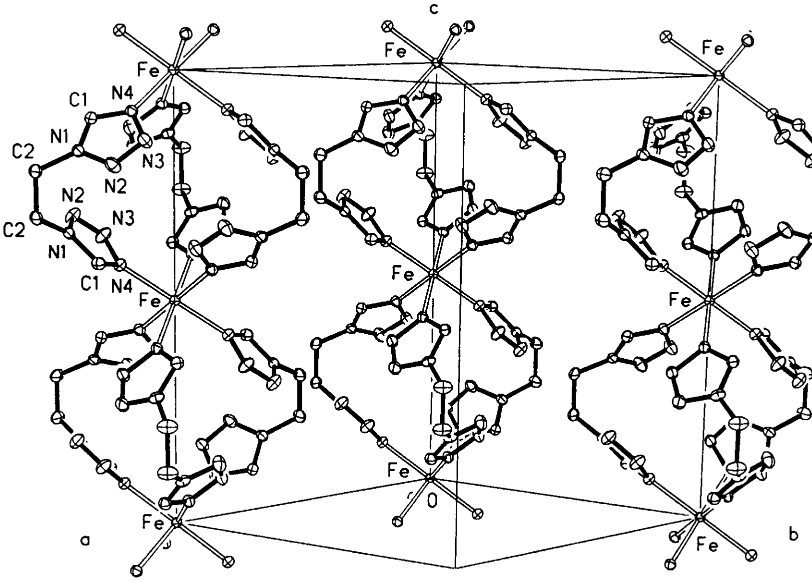

Fig. 7. Projection showing the unit cell of $[\mathrm{Fe}(\mathit{btze})_3](\mathrm{BF}_4)_2$. Alternative orientation of the chains defined by primed atoms (see Fig. 6) is omitted for clarity [25]

crystallographic *c*-axis, as depicted in Fig. 7. Naturally, the Fe(II) spin-crossover behaviour is also reflected in the Fe...Fe separations, which are 7.477, 7.461, 7.376 and 7.293 Å at 296, 200, 150 and 100 K, severally. In the *ab* plane the linear chains are arranged in a hexagonal close-packed fashion, creating channel-like spaces between them and occupied by the tetrahedral BF_4^- anions (Fig. 8).

Structure of $[\mathrm{Cu}(\mathit{btze})_3](\mathrm{ClO}_4)_2$

The crystal structure determination of $[\mathrm{Cu}(1,2\text{-bis(tetrazol-1-yl)ethane})_3](\mathrm{ClO}_4)_2$ carried out at 298 K also revealed a linear chain structure [26], which, however, shows important differences with respect to the one for the Fe(II) tetrafluoroborate derivative [25]. Interestingly, the Cu(II) compound crystallises in the orthorhombic space group Pbcn, whereas both Fe(II) linear chain compounds crystallise in the trigonal space group P$\bar{3}$c1 [24, 25]. Therefore, the Cu(II) chain lacks the threefold symmetry about the chain axis, which implies that the perfect octahedral symmetry about the metal(II) center is not conserved anymore. Indeed, the Cu(II) ions are in a *Jahn-Teller* distorted octahedral environment (Cu(1)–N(11) = 2.034(2) Å, Cu(1)–N(21) = 2.041(2) Å and Cu(1)–N(31) = 2.391(2) Å). The N–Cu–N angles are close to 90°, varying from 88.07(7) to 91.93(7)°. Furthermore, in contrast to $[\mathrm{Fe}(\mathit{btze})_3](\mathrm{BF}_4)_2$ there is only one crystallographic orientation for each *btze* ligand. The Cu(II) ions are linked by three *N*4, *N*4′ coordinating bis(tetrazole) ligands leading to a regular linear chain running along the *c*-axis, as displayed in Fig. 9. The *btze* ligands have a bent *syn* conformation which is shown by the torsion angles $\mathrm{N(14)–C(16)–C(16)^2–N(14)^2}$ of $-51.1(2)°$ and $\mathrm{N(24)–C(26)–C(36)^2–N(34)^2}$ of $-37.1(3)°$ (symmetry operation 2: $1-x$, y, $3/2-z$). It can noticed that the long Cu–N distance is compensated by a smaller torsion angle, in order to

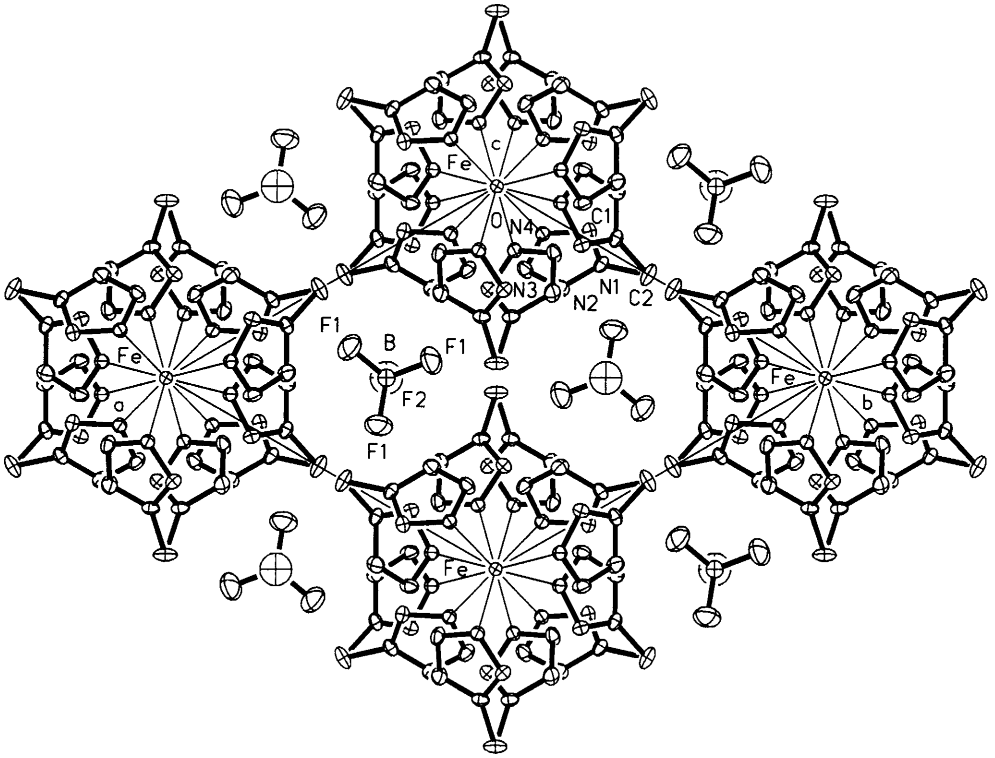

Fig. 8. Projection of the structure of [Fe(*btze*)$_3$](BF$_4$)$_2$ down the *c*-axis [25]

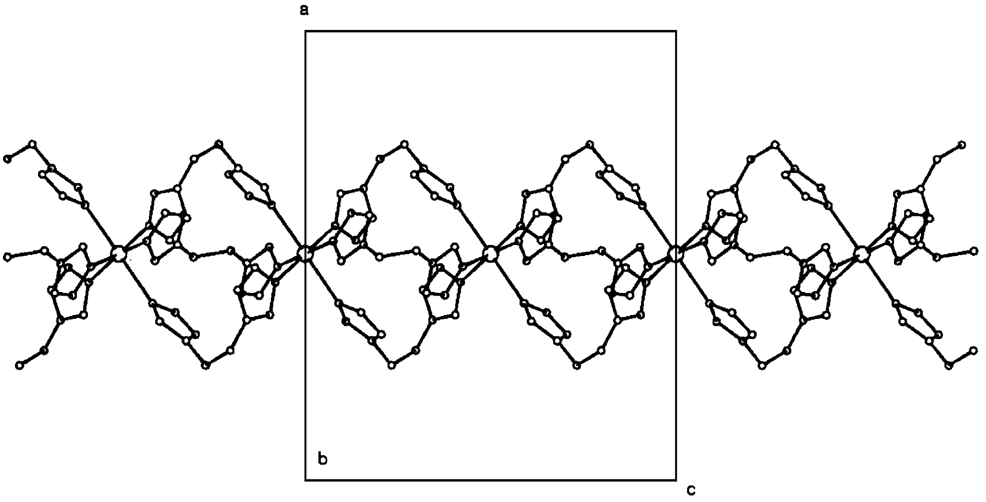

Fig. 9. Projection of the structure of [Cu(*btze*)$_3$](ClO$_4$)$_2$ along the *c*-axis [26]

allow the three ligands to fit in the linkage between the Cu ions. The N(24)–C(26)–C(36)^2–N(34)^2 torsion angle of $-37.1(3)°$ (symmetry operation 2: $1-x, y, 3/2-z$) is comparable to those observed for [Fe(1,2-bis(tetrazol-1-yl)propane)$_3$](ClO$_4$)$_2$ of $-34(1)°$ at 200 K and $-35(1)°$ at 100 K [24]. These features lead to a Cu…Cu separation of 7.420(3) Å, *i.e.* only slightly shorter than the Fe...Fe separations in the Fe(II) linear chain spin-crossover compounds in the high-spin form [24, 25]. The crystal packing of all three linear chain compounds discussed above is essentially identical, notwithstanding the fact that there are neither significant intermolecular contacts between the linear chains, nor hydrogen bonding interactions present in the structures.

Spin-Crossover Behaviour and Structures of [M(btzb)$_3$](ClO$_4$)$_2$ (M(II) = Fe, Cu)

Continuing our strategy of applying the linkage of tetrazole moieties by alkyl groups in order to obtain polynuclear iron(II) spin-crossover materials, the length of the alkyl spacer was varied. This yielded a class of threefold interlocked 3-D catenanes of formula [M(1,4-bis(tetrazol-1-yl)butane)$_3$](ClO$_4$)$_2$ (M(II) = Fe, Ni, Cu) [27]. The highly thermochromic polynuclear compound [Fe(1,4-bis(tetrazol-1-yl)butane)$_3$](ClO$_4$)$_2$ has been obtained in the form of colourless crystals. This feature arises from the fact that the spin-allowed *d–d* transition of lowest energy of the compound in the high-spin state, $^5T_{2g} \rightarrow {}^5E_g$, occurs in the near infrared region. Upon cooling, the colour changes to an intense pink. This is due to the $^1A_{1g} \rightarrow {}^1T_{1g}$ *d–d* transition of the compound in the low-spin state. The results of the variable temperature optical measurements are displayed in Fig. 10. Upon cooling, a very abrupt high-spin → low-spin transition taking place at 155 K is observed. Subsequent heating shows the low-spin → high-spin transition at 180 K, yielding a thermal hysteresis of 25 K. Further heating-and-cooling cycles within the temperature range 77–298 K indicate that this hysteresis is retained. It is worth noting that these measurements provide an accurate determination of the transition temperatures, but do not give any information on the population of the active spin-crossover sites, *i.e.* the percentage of iron(II) ions involved in the spin transition. The magnetic susceptibility measurements revealed that only *ca.* 16% of the Fe(II) ions are involved in the spin transition, characterized by $T_{1/2}\downarrow = 150$ K and $T_{1/2}\uparrow = 170$ K. This hysteresis of 20 K has been reproduced along several thermal cycles. The

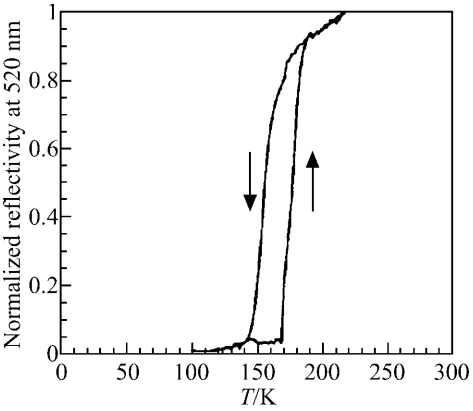

Fig. 10. Optical detection of the spin transition for [Fe(*btzb*)$_3$](ClO$_4$)$_2$ [27]

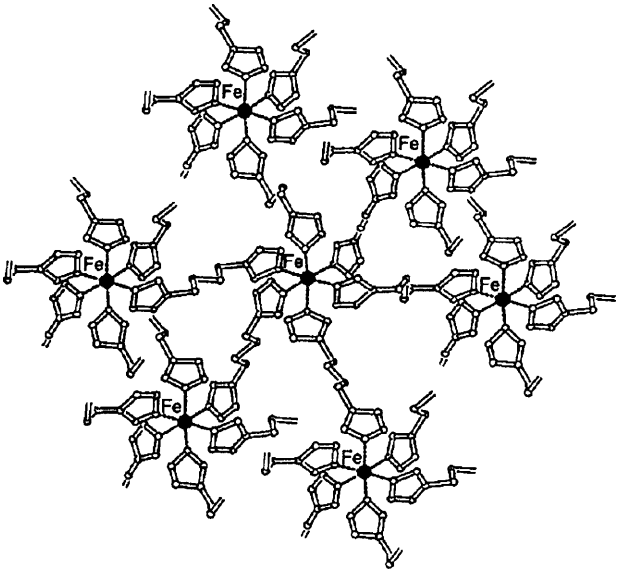

Fig. 11. Tentative 3-D model (150 K) for [Fe(*btzb*)$_3$](ClO$_4$)$_2$ [27]

slight discrepancy between the transition temperatures determined by optical and magnetic methods is most likely related to different sample – thermal response/ temperature detector geometries in both applied techniques. The optical measurements focus on the colour, *i.e.* the surface of the sample, whereas the magnetic data reflect the physical behaviour of the bulk material [28, 29].

Furthermore, irradiation with green light at 30 K lead to the population of the metastable high-spin state for the thermally active iron(II) ions. Therefore, [Fe(btzb)$_3$](ClO$_4$)$_2$ represents the first 3-D Fe(II) spin-crossover material displaying the LIESST effect.

Unfortunately, only a tentative model of the 3-D structure of [Fe(*btzb*)$_3$](ClO$_4$)$_2$ at 150 K could be determined (Fig. 11). Each of the ligands is located on an inversion centre. This causes all central C–C linkages to be in the *anti* conformation. Of the six independent N–C–C–C torsions in the ligands, four are also in the *anti* conformation, but two fit the electron density best when brought into a *gauche* conformation. A detailed reanalysis of the crystallographic data has been carried out recently [30]. This revealed a model showing three symmetry related, interpenetrating, 3-D Fe–*btzb* networks. Iron atoms within one network are separated by the unit cell translations. The iron atoms of two non-connected networks approach each other as close as 8.3 and 9.1 Å according to this model. The crystal structure of the Cu(II) analogue confirmed this threefold interpenetrating 3-D catenane structure [31]. The driving force for the formation of these unprecedented supramolecular 3-D catenane materials lies in the conformation adopted by the alkyl spacer used to link the tetrazole moieties. Upon increasing of the spacer length the *anti* conformation, as has been found for the free *btzb* and for the Fe(II) catenane of *btzb* [27], is favoured over the bent *syn* conformation as found in the linear chains of ligands with smaller spacers [24–26].

Discussion

[Fe(*btzb*)$_3$](ClO$_4$)$_2$ is the first Fe(II) spin-crossover material with a supramolecular catenane structure consisting of three interlocked 3-D networks. Although, especially during the past few years several new polynuclear Fe(II) spin-crossover compounds have been reported (*vide infra*), the structure of the present compound is highly novel [27, 30]. Its structure is built up from three interlocked crystallographically dependent 3-D [Fe(*btzb*)$_3$]$^{2+}$ networks [30]. From the disorder met in this structure, it is evident that the crystal lattice does not involve the most efficient packing. In fact, it appears that in [Fe(*btzb*)$_3$](ClO$_4$)$_2$ four of the six crystallographically independent *btzb* ligands are in an *anti* conformation, whereas the remaining two are in a *syn* conformation. Interestingly, the crystal structure determination did not reveal any well-defined type of intra- or intermolecular interaction, which could be responsible for the stabilization of this unusual supramolecular structure.

A comparison may be made with the first supramolecular 2-D catenane exhibiting thermal spin-crossover behaviour [32]. The structure of [Fe(*tvp*)$_2$(NCS)$_2$] · CH$_3$OH (*tvp* = 1,2-di-(4-pyridyl)-ethylene) has been elucidated at room temperature and consists of two interpenetrating two-dimensional [Fe(*tvp*)$_2$(NCS)$_2$] sheets. The octahedrally coordinated Fe(II) ion contains two thiocyanate anions in *trans* positions, whereas the four surrounding bidentate N-coordinating *tvp* ligands link the Fe(II) ions into 2-D layers. The Fe...Fe separation through the *tvp* ligand is 13.66 Å. The Fe...Fe separations involving metal ions originating from interpenetrating layers are 22.59 and 15.36 Å. The difference in ligand dimensions between *tvp* and *btzb*, leads to a somewhat larger Fe...Fe separation over the direct *btzb* linkage, *i.e. ca.* 15 Å. However, the interweaving of three 3-D lattices gives rise to extremely short Fe...Fe separations of 8.3 and 9.1 Å between symmetry related non-connected lattices.

The same group pursued this research and reported on the threefold interlocked 2-D catenane system [Fe(*bpb*)$_2$(NCS)$_2$] · 0.5CH$_3$OH (*bpb* = 1,4-bis(4-pyridyl)-butadiyne) [33]. The structure consists of 2-D [FeL$_2$(NCS)$_2$] sheets comparable to the ones found in the former material, however, because of the increased rigidity and larger size of the present *bpb* ligand, now three mutually perpendicular nets are intercatenated. The crystal structure involves two symmetry independent networks leading to Fe...Fe separations over the direct *bpb* linkage of 16.628 Å and 16.393 Å, respectively.

The only other Fe(II) spin-crossover compound having a 3-D lattice with which comparisons may be made is [Fe(*btr*)$_3$](ClO$_4$)$_2$ (*btr* = 4,4′-bis-1,2,4-triazole) [34]. This compound may be regarded as a 3-D analogue of the 2-D spin-crossover materials [Fe(*btr*)$_2$(NC*X*)$_2$] (*btr* = 4,4′-bis-1,2,4-triazole; *X* = S [35], or Se [36]). The latter systems were first reported 15 years ago, and solely by incorporating the non-coordinating anion perchlorate for the N-coordinating thiocyanate anion, the 3-D Fe(II) spin-transition compound has been obtained. The structure of [Fe(*btr*)$_3$](ClO$_4$)$_2$ [34] was solved at 150, 190 and 260 K and comprises a 3-D network in which the crystallographically independent Fe1 and Fe2 ions are connected by single μ-*N*1,*N*1′-4,4′-bis-1,2,4-triazole bridges. Since the rather rigid *btr* ligand is smaller than the *btzb* ligand, the metal-metal separations over the bridging *btr* ligands are considerably shorter than for $[Fe(btzb)_3](ClO_4)_2$, *i.e.* Fe1…Fe2 (both in the HS form) = 8.67 Å at 260 K, Fe1 (HS)…Fe2 (LS) = 8.55 Å at 190 K, and Fe1…Fe2 (both in the LS form) = 8.42 Å at 150 K. Interestingly, these values are of the same order as the Fe…Fe spacings of 8.3 and 9.1 Å between different nets, *i.e.* through space, in the *btzb* material.

It is believed that the direct connectivity of the Fe(II) sites in polynuclear Fe(II) spin-transition compounds may have a favourable effect on the strength of the elastic interactions between the active Fe(II) spin-crossover centers, thereby increasing the cooperativity of the spin transition, leading to very abrupt spin-crossover behaviour. Indeed, this appears to be the case for the series of linear chain compounds of formula $[Fe(4\text{-}R\text{-}trz)_3](anion)_2 \cdot xH_2O$ (4-*R*-*trz* = 4-substituted-1,2,4-triazole) [1–3, 7, 9–11, 28, 37–40], where the direct linkage of the Fe(II) spin-crossover centers by triple *N*1,*N*2-1,2,4-triazole bridges is assumed to account for the cooperative nature of the spin transition. When the ligand spacer linking the Fe(II) ions becomes more flexible, as is the case for $[Fe(1,2\text{-bis(tetrazol-1-yl)propane})_3](ClO_4)_2$ [24] and $[Fe(1,2\text{-bis(tetrazol-1-yl)ethane})_3](ClO_4)_2$ [25], the spin-crossover behaviour becomes more gradual. This is the signature for the negligible magnitude of the elastic interactions, which is most probably due to the 1,2-propane or 1,2-ethylene unit acting as some kind of shock absorber of the elastic interactions. This may be further illustrated by a comparison of the structures of $[Cu(hyetrz)_3](ClO_4)_2 \cdot 3H_2O$ (*hyetrz* = 4-(2′-hydroxy-ethyl)-1,2,4-triazole) [41] and $[Cu(btze)_3](ClO_4)_2$ [26]. The structure of $[Cu(hyetrz)_3](ClO_4)_2 \cdot 3H_2O$ shows Cu(II) ions linked by triple *N*1,*N*2 1,2,4-triazole bridges yielding an unsymmetrical chain with two different alternating copper–copper distances, *i.e.* Cu1–Cu2 = 3.853(2) Å and Cu2–Cu3 = 3.829(2) Å, respectively. It is important to notice that even though the Cu(II) ions are in *Jahn-Teller* distorted octahedra, the chain shows only a relatively small deviation from linearity [41]. For $[Cu(btze)_3](ClO_4)_2$, in spite of the *Jahn-Teller* distorted geometry about the Cu(II) ions, the chain does not show any deviation from linearity [26]. Obviously, the flexibility of the ethylene linkage allows the preservation of the perfect linear chain structure, since the *Jahn-Teller* deformation of the Cu(II) coordination sphere has been successfully compensated by important variations in the N–C–C–N torsion angles of the *btze* ligands.

The same type of reasoning concerning the shock-absorbing properties of the direct bridging ligand may be applied to $[Fe(tvp)_2(NCS)_2] \cdot CH_3OH$ [32] and $[Fe(bpb)_2(NCS)_2] \cdot 0.5CH_3OH$ [33], which show only a very gradually proceeding and incomplete spin transition. Although the 1,2-di-(4-pyridyl)-ethylene and 1,4-bis(4-pyridyl)-butadiyne ligands themselves may *a priori* not be considered as flexible, it seems that the negligible magnitude of the elastic interactions is brought about by the flexibility of the 2-D network itself. This is illustrated by the absence of significant intra- and intermolecular interactions, which leads to the formation of large channels between the interlocked lattices.

On the other hand, both 3-D Fe(II) spin-crossover compounds show abrupt spin-crossover behaviour. The crystal structure of $[Fe(btr)_3](ClO_4)_2$ revealed the presence of two slightly different Fe(II) spin-crossover sites, each displaying its own magnetic behaviour [34]. This leads to a two-step spin conversion with 50% of the Fe(II) ions (site Fe1) undergoing a very abrupt spin transition with a small hysteresis of 3 K centered at 184 K, whereas the other 50% of Fe(II) ions (site Fe2) display rather gradual spin-crossover behaviour with $T_{1/2} = 222$ K.

The structural model for [Fe(*btzb*)$_3$](ClO$_4$)$_2$ showed three interlocked 3-D [Fe(*btzb*)$_3$]$^{2+}$ lattices [27, 30]. At 150 K, the Fe(II) ions of two non-connected networks approach each other as close as 8.3 and 9.1 Å. These distances involving no direct bridging ligands are comparable to the Fe1...Fe2 separation within [Fe(*btr*)$_3$](ClO$_4$)$_2$, albeit over a direct *btr* linkage [34]. Interestingly, the spin-crossover behaviour of [Fe(*btzb*)$_3$](ClO$_4$)$_2$ is far more abrupt with transition temperatures $T_{1/2}\uparrow = 170$ K and $T_{1/2}\downarrow = 150$ K, *i.e.* involving a rather large thermal hysteresis of about 20 K for a small fraction of *ca.* 16% of the Fe(II) ions involved in this transition; the remaining Fe(II) ions stay in the HS state [27]. It is worth noting that this is the largest thermal hysteresis observed up to now for iron(II) tetrazole derivatives. Apparently, the rigidity originating from the interweaving within this threefold 3-D interlocked lattice, is responsible for the efficient propagation of the elastic interactions leading to this type of cooperative spin-crossover behaviour. However, the same factors may also be invoked for explaining the small fraction of Fe(II) ions undergoing the spin transition. Most probably, the structural changes accompanying the Fe(II) spin transition modify the structure in such a way that the further spin-crossover of the high-spin Fe(II) ions upon cooling is severely hampered.

Conclusion

The comparison of these various polynuclear Fe(II) spin-crossover compounds has revealed that the predominant factor related to the cooperativity of the spin-crossover behaviour is neither the Fe...Fe separation, nor the dimensionality of the Fe(II) spin transition material, but rather the stiffness and rigidity with which the Fe(II) centers are maintained within the crystal lattice. Up to now, it has been observed that this rigidity may either arise from the stiffness of the direct bridges between the active spin-crossover centers as found in the linear chain materials [Fe(4-*R*-*trz*)$_3$](anion)$_2 \cdot x$H$_2$O [1–3, 7, 9–11, 28, 37–40], or from the efficient crystal packing of the lattice itself, as demonstrated for the 3-D spin-crossover material [Fe(*btzb*)$_3$](ClO$_4$)$_2$ [27, 30].

For the Fe(II) linear chain spin-transition materials, it is generally agreed upon that the cooperative Fe(II) spin-crossover behaviour of the Fe(II) 4*R*-1,2,4-triazole linear chains is related to the tight linking of the active Fe(II) centers by triple *N*1,*N*2 1,2,4-triazole bridges. On the other hand, the crucial factor responsible for the cooperative Fe(II) spin-crossover behaviour for the 3-D supramolecular catenane [Fe(*btzb*)$_3$](ClO$_4$)$_2$ [27] is the closed 3-D packing of the whole coordination polymer, and is certainly not caused by the rather flexible bridging *btzb* ligand itself.

It appears that the difference in dimensionality of the Fe(II) spin transition materials may be relevant to important variations in the response of the crystal lattice towards the Fe(II) spin-crossover. It becomes evident from the structural data of [Fe(*btzp*)$_3$](ClO$_4$)$_2$ [24] and [Fe(*btze*)$_3$](BF$_4$)$_2$ [25] that the main structural changes occurring during the spin transition are directed along the chain axis. Concomitant with this, the change in unit-cell dimensions predominantly takes place along the *c*-axis; therefore, the volume change upon spin-crossover is extremely anisotropic. The magnitude of the thermal contraction upon the Fe(II) spin transition could not be determined for the Fe(II) spin-crossover linear chain compounds of 4-*R*-1,2,4-triazole, since no structural data are available. Fe(II) spin transition materials of higher dimensionality may have more favourable thermal expansion characteristics upon Fe(II) spin-crossover. In these compounds, the change in unit-cell volume will occur more or less uniformly in all directions. Therefore, the elastic interactions are also expected to be more isotropic. Preliminary results have already confirmed this for another threefold interlocked 3-D supramolecular Fe(II) catenane of *btzb* [42].

Clearly, the family of α,β- and α,ω-bis(tetrazol-1-yl)alkane type ligands have been very valuable building blocks in the Fe(II) spin-crossover research. This approach already lead to the first structurally characterized 1-D iron(II) spin-crossover compound. This same [Fe(*btzp*)$_3$](ClO$_4$)$_2$ was also the first linear chain Fe(II) spin-crossover material to show the LIESST effect [24]. Furthermore, [Fe(*btzb*)$_3$](ClO$_4$)$_2$ represents the first supramolecular catenane Fe(II) spin-crossover compound with three interlocked 3-D networks. This thermochromic material can be switched by both temperature and light [27].

Further research on this type of polytetrazole systems is currently being carried out. Variation in the synthetic route provides a solid basis for tuning the spin-crossover behaviour by modifying the nature of the spacer between the tetrazole entities. In this way, a systematic tuning of the Fe...Fe separation is achieved, and more importantly, the dimensionality of the Fe(II) spin-crossover system can be changed.

Acknowledgements

For the supportive fruitful discussions we want to express our thank to *Kurt Mereiter* of the Institute of Chemical Technologies and Analytics of the Vienna University of Technology. This work was partly funded by the European Union within the TMR Research Network ERB-FMRX-CT98-0199 entitled "Thermal and Optical Switching of Molecular Spin States (TOSS)", the European Science Foundation program "Molecular Magnets" and the Hochschuljubiläumsfonds der Stadt Wien project H-65/2000.

References

[1] Kahn O, Jay-Martinez C (1998) Science **279**: 44
[2] Kahn O, Kröber J, Jay C (1992) Adv Mater **4**: 718
[3] Jay C, Grolière F, Kahn O, Kröber J (1993) Mol Cryst Liq Cryst **234**: 255
[4] Gütlich P (1981) Struct Bonding (Berlin) **44**: 83
[5] Zarembowitch J, Kahn O (1991) New J Chem **15**: 181
[6] König E (1987) Prog Inorg Chem **35**: 527
[7] Haasnoot JG (1996) In: Kahn O (ed) Magnetism: A Supramolecular Function. Kluwer, Dordrecht, 299
[8] Gütlich P, Garcia Y, Goodwin HA (2000) Chem Soc Rev **29**: 419
[9] Kahn O, Codjovi E (1996) Phil Trans R Soc London A **354**: 359
[10] Kahn O, Codjovi E, Garcia Y, van Koningsbruggen PJ, Lapouyade R, Sommier L (1996) In: Turnbull MM, Sugimoto T, Thompson LK (eds) Molecule-Based Magnetic Materials, Symposium Series No. 644, American Chemical Society, Washington, DC, 298

[11] Haasnoot JG (2000) Coord Chem Rev **200–202**: 131

[12] Gütlich P, Hauser A (1990) Coord Chem Rev **97**: 1

[13] Gütlich P, Hauser A, Spiering H (1994) Angew Chem Int Ed Engl **33**: 2024

[14] Gütlich P, Jung J, Goodwin HA (1996) NATO ASI Series. Kluwer, Dordrecht, p 327

[15] Gütlich P (1997) Mol Cryst Liq Cryst **305**: 17

[16] a) Franke PL, Haasnoot JG, Zuur AP (1982) Inorg Chim Acta **59**: 5; b) Müller WE, Ensling J, Spiering H, Gütlich P (1983) Inorg Chem **22**: 2074

[17] Wiehl L (1993) Acta Crystallogr **B49**: 289

[18] a) Sanner I, Meißner E, Köppen H, Spiering H (1984) Chem Phys **86**: 227; b) Willenbacher N, Spiering H (1988) J Phys C: Solid State Phys **21**: 1423; c) Spiering H, Willenbacher N. (1989) J Phys Condens Matter **1**: 10089

[19] Jung J, Schmitt G, Wiehl L, Hauser A, Knorr K, Spiering H, Gütlich P (1996) Z Phys B **100**: 523

[20] Sorai M, Ensling J, Hasselbach KM, Gütlich P (1977) Chem Phys **20**: 197

[21] a) Buchen T, Gütlich P, Sugiyarto KH, Goodwin HA (1996) Chem Eur J **2**: 1134; b) Sugiyarto KH, Weitzner K, Craig DC, Goodwin HA (1997) Aust J Chem **50**: 869

[22] a) Letard JF, Guionneau P, Codjovi E, Lavastre O, Bravic G, Chasseau D, Kahn O (1997) J Am Chem Soc **119**: 10861; b) Letard JF, Guionneau P, Rabardel L, Howard JAK, Goeta AE, Chasseau D, Kahn O (1998) Inorg Chem **37**: 4432

[23] a) Zhong ZJ, Tao JQ, Yu Z, Dun CY, Liu YJ, You XZ (1998) J Chem Soc Dalton Trans 327; b) Boca R, Boca M, Dlhán L, Falk K, Fuess H, Haase W, Jarošciak R, Papánková B, Renz F, Vrbová M, Werner R (2001) Inorg Chem **40**: 3025

[24] van Koningsbruggen PJ, Garcia Y, Kahn O, Fournès L, Kooijman H, Haasnoot JG, Moscovici J, Provost K, Michalowicz A, Renz F, Gütlich P (2000) Inorg Chem **39**: 891

[25] Schweifer J, Weinberger P, Mereiter K, Boca M, Reichl C, Wiesinger G, Hilscher G, van Koningsbruggen PJ, Kooijman H, Grunert M, Linert W (2002) Inorg Chim Acta (accepted)

[26] van Koningsbruggen PJ, Garcia Y, Bravic G, Chasseau D, Kahn O (2001) Inorg Chim Acta **326**: 101

[27] van Koningsbruggen PJ, Garcia Y, Kooijman H, Spek AL, Haasnoot JG, Kahn O, Linares J, Codjovi E, Varret F (2001) J Chem Soc Dalton Trans 466

[28] van Koningsbruggen PJ, Garcia Y, Codjovi E, Lapouyade R, Kahn O, Fournès L, Rabardel L (1997) J Mater Chem **7**: 2069

[29] a) Varret F, Constant-Machado H, Dormann JL, Goujon A, Jeftic J, Noguès M, Bousseksou A, Klokishner S, Dolbecq A, Verdaguer M (1998) Hyperfine Interact **113**: 37; b) Morscheidt W, Codjovi E, Jeftic J, Linarès J, Bousseksou A, Constant-Machado H, Varret F (1998) Meas Sci Technol **9**: 1311; c) Codjovi E, Morscheidt W, Jeftic J, Linarès J, Nogues M, Goujon A, Roubeau O, Constant-Machado H, Desaix A, Bousseksou A, Verdaguer M, Varret F (1999) Mol Cryst Liq Cryst **335**: 1295

[30] Mereiter K, Kooijman H, van Koningsbruggen PJ, Grunert M, Weinberger P, Linert W (2002) (unpublished results)

[31] van Koningsbruggen PJ, Bravic G, Chasseau D, Mereiter K, Grunert M, Weinberger P, Linert W (in preparation)

[32] Real JA, Andrés E, Munoz MC, Julve M, Granier T, Bousseksou A, Varret F (1995) Science **268**: 265

[33] Moliner N, Muñoz C, Létard S, Soans X, Menéndez N, Goujon A, Varret F, Real JA (2000) Inorg Chem **39**: 5390

[34] Garcia Y, Kahn O, Rabardel L, Chansou B, Salmon L, Tuchagues JP (1999) Inorg Chem **38**: 4663

[35] a) Vreugdenhil W, Haasnoot JG, Kahn O, Thuéry P, Reedijk J (1987) J Am Chem Soc **109**: 5272; b) Vreugdenhil W, van Diemen JH, de Graaff RAG, Haasnoot JG, Reedijk J, van der Kraan AM, Kahn O, Zarembowitch J (1990) Polyhedron **9**: 2971

[36] Ozarowski A, Shunzhong Y, McGarvey BR, Mislankar A, Drake JE (1991) Inorg Chem **30**: 3167

[37] a) Lavrenova LG, Ikorskii VN, Varnek VA, Oglezneva IM, Larionov SV (1986) Koord Khim **12**: 207; b) Lavrenova LG, Ikorskii VN, Varnek VA, Oglezneva IM, Larionov SV (1990) Koord Khim **16**: 654; c) Lavrenova LG, Yudina NG, Ikorskii VN, Varnek VA, Oglezneva IM, Larionov SV (1995) Polyhedron **14**: 1333

[38] Codjovi E, Sommier L, Kahn O, Jay C (1996) New J Chem **20**: 503

[39] a) Garcia Y, van Koningsbruggen PJ, Codjovi E, Lapouyade R, Kahn O, Rabardel L (1997) J Mater Chem **7**: 857; b) Garcia Y, van Koningsbruggen PJ, Lapouyade R, Fournès L, Rabardel L, Kahn O, Ksenofontov V, Levchenko G, Gütlich P (1998) Chem Mater **10**: 2426

[40] Garcia Y, van Koningsbruggen PJ, Lapouyade R, Rabardel L, Kahn O, Wieczorek M, Bronisz R, Ciunik Z, Rudolf MF (1998) C R Acad Sci Paris **II c**: 523

[41] Garcia Y, van Koningsbruggen PJ, Bravic G, Guionneau P, Chasseau D, Cascarano GC, Moscovici J, Lambert K, Michalowicz A, Kahn O (1997) Inorg Chem **36**: 6357

[42] Grunert M, Schweifer J, Weinberger P, Mereiter K, Boca M, Hilscher G, van Koningsbruggen PJ, Linert W (in preparation)